Facies (2025) 71:2
https://doi.org/10.1007/s10347-024-00692-z

ORIGINAL ARTICLE

Census-based estimates of Mediterranean Oligocene–Miocene reef carbonate production

Wolfgang Kiessling[1] · Danijela Dimitrijević[1] · Nussaïbah B. Raja[1] · Kerstin Frühbeißer[1] · Alessandro Vescogni[2] · Francesca R. Bosellini[2]

Received: 12 September 2024 / Accepted: 4 November 2024

Abstract
Census-based approaches to reefal carbonate budgets are increasingly being used to project the near-future fate of tropical coral reefs. Some of the census parameters are difficult to achieve in fossil reef systems, which may be the reason why no census-based estimates of fossil reef carbonate production have been published until now. Here, we apply a census-based estimate of gross carbonate production in two reef systems from southeastern Italy to (1) test if reasonable estimates are possible and (2) assess the variability of carbonate production rates over time and reef environment. We confirm that estimates of late Oligocene and late Miocene reef gross carbonate production are within the range of modern coral reefs with the late Oligocene reef front showing the greatest carbonate production (6.1 ± 1.3 kg $CaCO_3$ m^{-2} $year^{-1}$) and the late Miocene reef front exhibiting the lowest production (1.7 ± 0.5 kg $CaCO_3$ m^{-2} $year^{-1}$). The decline of reef carbonate production from the Oligocene to the Miocene is accompanied by a decline of reef builder biodiversity but driven by the lower coral cover and coral growth rates in the Miocene. The decline of reefal carbonate production may be related to late Cenozoic cooling.

Keywords Reefs · Carbonate budget · Corals · Growth rates · Oligocene · Miocene · Climate change

Introduction

Suffering from direct human impacts and climate change, several modern tropical coral reefs have low or even negative accretion rates (i.e., erosion surpassing reef growth), which renders them vulnerable to near-future sea-level rise (Perry et al. 2018). Although sea-level rise is unlikely to lead to complete reef drowning within centuries, evidence from the geological past confirms that the drowning of reefs and carbonate platforms was a widespread phenomenon. The exact interplay between the rate of sea-level rise and reef growth rate is difficult to constrain in the geological record (Schlager 1981). This difficulty is partly due to the timescale dependence of most rates that are observed in nature.

For example, there is a power-law relationship between the timespan of observation and measured sediment accumulation rates and reef growth rates (Sadler 1981; Schlager 1999; Kemp 2012). The scaling effect is mainly due to hiatuses or times of slow accumulation, which intervene with times of rapid sediment accumulation or reef accretion. Scale-dependency is a considerable problem for comparing past and present accretion rates. Dividing the thickness of a reef by the timespan over which the reef grew will lead to severely underestimated maximum reef accretion rates.

Census-based estimates of reefal carbonate production are quantified from the reef biota coverage and their growth rates (Lange et al. 2020). Unlike other estimates of net accretion rates, the census-based approach is designed to provide a snapshot estimate of reef growth capacity and is thus not prone to the scaling effect. Comparing carbonate production rates across sites can thus provide insights into optimal growth conditions or reef health. A carbonate budget is the quantitative assessment of the inputs and outputs of carbonate within the active carbonate-producing environment and is typically expressed as a measure in kg $CaCO_3$ m^{-2} $year^{-1}$ (Perry 2011).

✉ Wolfgang Kiessling
wolfgang.kiessling@fau.de

[1] Department of Geography and Geosciences, GeoZentrum Nordbayern, Friedrich-Alexander-Universität Erlangen-Nürnberg, Erlangen, Germany

[2] Dipartimento di Scienze Chimiche e Geologiche, Università di Modena e Reggio Emilia, Modena, Italy

Published online: 09 December 2024

Establishing the carbonate budget of reefs has a long tradition (Chave et al. 1972; Hubbard et al. 1990), and census-based budgets have now reached methodological maturity (Perry et al. 2008, 2012, 2015, 2018). The most important variables determining gross production are calcification rates, life cover, and reef rugosity. Rugosity is a measure of topographic complexity. Life cover refers to any reef builder, in Cenozoic reefs usually stony corals and crustose coralline algae (Perrin and Kiessling 2010). Similarly, calcification rate refers to the calcification of the prevailing reef builders, which depends on growth rate and skeletal density (Lough 2008; Lough and Cooper 2011). Importantly, reef growth is only weakly tied to coral growth (Dullo 2005) and even reefs dominated by fast-growing corals can suffer from a negative carbonate budget (Edinger et al. 2000). Losses of carbonate due to bioerosion and mechanical breakdown are also part of the reef budget controlling the net accumulation and thus actual reef growth.

Here, we apply for the first time a census-based reef budget approach to fossil reefs. We studied two Cenozoic reef systems in southeastern Italy to showcase the applicability of the method and its limitations. The method yields reasonable estimates of gross carbonate production and can potentially be applied to other fossil reefs as well.

Materials and methods

Geological setting

We studied two reef systems in Salento, Apulia, southeastern Italy (Fig. 1), which developed along the eastern margin of the Apulia Platform (Bosellini et al. 1999). The older reef system is of late Oligocene (middle-late Chattian) age, whereas the younger reef system belongs to the late Miocene (early Messinian) age.

The Oligocene reef system is represented by the Castro Limestone and has been mainly interpreted as a fringing reef (Bosellini and Russo 1992; Bosellini et al. 2002, 2021; Bosellini 2006), albeit with a distinct backreef lagoon. The thickness of this Chattian reef complex ranges from a minimum of 5 m on the platform top to a maximum of about 80–100 m along the slope, depending on the available accommodation space at the time of deposition. The reef shows a well-preserved lateral zonation of reef subenvironments across its profile: a lagoonal back reef, a reef flat, a reef front, and finally a reef slope (Fig. 1).

The Miocene reef system is represented by the Novaglie Formation and is largely constructed by a single genus of reef corals: *Porites* (Bosellini et al. 2001). *Porites* colonies are columnar or massive and accompanied by coralline algae, encrusting foraminifera, vermetids, and bryozoans (Bosellini 2006). The Messinian slope reefs are constructed

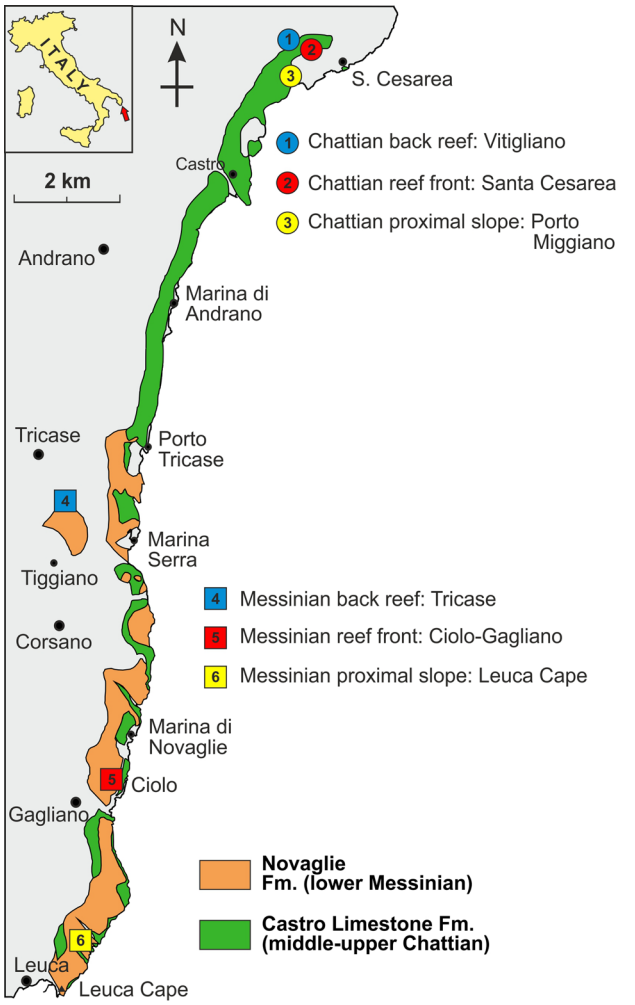

Fig. 1 Study sites in Salento (Apulia, Italy). The Oligocene (Chattian) sites are indicated with circles, the Miocene (Messinian) sites with squares

by the same organisms as the more proximal reefs, but additional components contributed to their construction, such as *Halimeda* (packstones and mounds), serpulids, bioclastic calcarenites, coral breccia, and rhodolite float- and rudstones.

The two fringing reef systems grew, in different times, along the eastern margin of the Apulia Platform, which remained stable and undeformed from the Cretaceous until the Late Miocene (Bosellini et al. 1999) (Fig. 2). Therefore, the physiographic setting was nearly identical, allowing a comparison not biased by different local depositional factors (Bosellini 2006).

Study sites

We studied six sites in detail, three from the Oligocene reef system and three from the Miocene (Fig. 1, Table 1). Sites

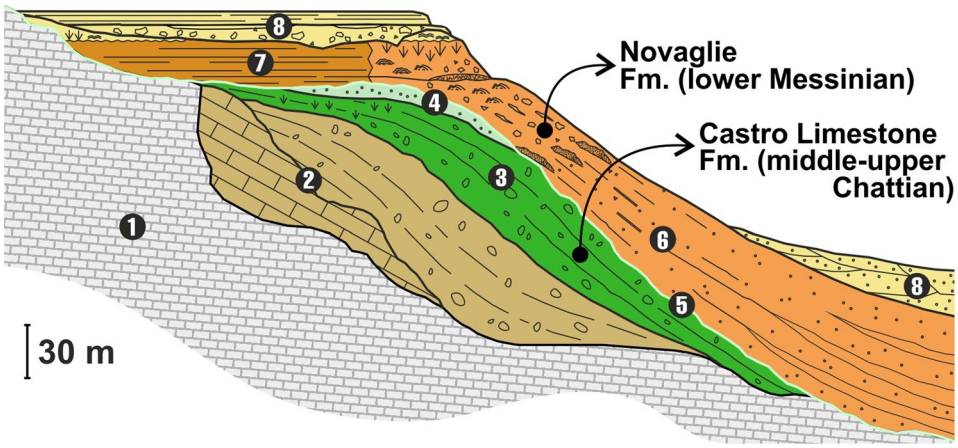

Fig. 2 Stratigraphic architecture of eastern Salento Peninsula (modified after Bosellini et al. 1999). (1) Upper Cretaceous substrate; (2) Eocene limestones; (3) Castro Limestone Fm. (middle-upper Chattian); (4) Uppermost Chattian limestones; (5) Serravallian-Tortonian hardground; (6) Novaglie Fm. (lower Messinian); (7) Andrano Calcarenites (lower Messinian); (8) Upper Messinian to Lower Pleistocene deposits (modified after Bosellini et al. 1999). Studied reef systems are from the Castro Formation and from the Novaglie Formation, respectively

Table 1 Names, reef area type and coordinates of the six locations where growth bands were measured. Colored locations are those that allowed a reconstruction of a reef budget

Locality	Reef area	Age	Number of line transects/rugosity measurements	Coordinates (latitude, longitude in decimal degrees)
Vitigliano (V)	Back reef	Oligocene (Chattian)	4/0	40.040, 18.417
Santa Cesarea (SC)	Reef front	Oligocene (Chattian)	8/10	40.040, 18.443
Porto Miggiano (PM)	Proximal reef slope	Oligocene (Chattian)	6/0	40.035, 18.445
Tricase (T)	Back reef	Miocene (Messinian)	6/0	39.922, 18.368
Ciolo - Gagliano del Capo (CG)	Reef front	Miocene (Messinian)	7/2	39.847, 18.385
Leuca cape (LC)	Proximal reef slope	Miocene (Messinian)	4/3	39.799, 18.372

have been selected to represent different reef environments, which can be found in both time slices. Reef framework was only encountered at three sites and we limit our census-based estimates of carbonate production to those three sites (Table 1).

Among the Oligocene sites, the backreef is best developed at a roadcut in Vitigliano, where scattered corals are in growth position within bioclastic packstones and grainstones. This site was suitable for line transects and growth rate analyses. The Oligocene reef front is beautifully exposed above Santa Cesarea in a roadcut. Here a nearly 6 m thick coral framework with large corals is preserved. The framework is locally quite dense (up to 64% of coral cover) and built by a diverse coral fauna (at least 13 genera recognized in the field) with dominantly massive growth forms and some coralline algae (Bosellini et al. 2021).

The proximal fore reef at Porto Miggiano is dominated by reworked coral colonies and fragments. Due to the lack of in-situ framework, we report coral growth rates but refrain from a carbonate budget assessment.

The corresponding Miocene sites were Tricase (backreef), Ciolo-Gagliano (reef front), and Leuca cape (proximal fore reef). Similar to the Oligocene, the backreef is dominated by sediment (marly in Tricase). Reef budgets were estimated in the reef front and proximal fore reef. The former (Ciolo-Gagliano) is characterized by massive and columnar *Porites* with high in-situ coral cover, whereas the latter (Leuca cape) is a *Porites* pillarstone. Work at Ciolo-Gagliano was difficult owing to a stone chip grid protecting the road.

Census approach

Census-based methods in reef systems estimate the carbonate production in kg m^{-2} $year^{-1}$ based on the growth density, growth rate and skeletal density of carbonate producing organisms. In addition, the morphological complexity of the reef framework (rugosity) is used as a multiplier. These variables can be evaluated with a large suite of methods one of which is the line intercept method, which is an accurate method to evaluate coral cover in living reefs (Jokiel et al. 2015) and can be applied in fossil reefs (Mewis and Kiessling 2013). We applied the equations of Perry et al. (2012) to estimate reef carbonate production rates. Because corals were the only prolific reef builders (see results), we equated coral production with reef production (P_g).

$$P_g = \Sigma\left(R \times \left(\left(X_i/100\right) \times \left(\left(D_i \times G_i \times 10,000\right)/1000\right)\right)\right), \quad (1)$$

where: R = Rugosity of transect, measured as the ratio of surface distance relative to linear distance, X_i = Mean % cover of *i*th coral species, D_i = Skeletal density (g cm^{-3}) of the *i*th species, G_i = Growth rate (cm $year^{-1}$) of the *i*th species, P_g is estimated in kg $CaCO_3$ m^{-2} $year^{-1}$.

To collect the required parameters, we used line transects to evaluate the coral cover and the ratio of the line length attached to a paleo-reef surface to the shortest distance as an estimate of reef rugosity. Coral growth rates were measured along transects (also outside transects but always within the same setting), whereas coral skeletal density could only be taken from the literature.

Mean by-species coral cover was assessed using line transects, performed with a 10 m long rope marked every 10 cm. The rope was fixed randomly across the reef outcrop at different horizons but was biased by accessibility. The components at every mark were identified and noted; unidentified components were disregarded. These data were used to calculate the coral cover percentage for each genus for each sampled reef site. Corals could usually only be identified to the genus level, which is our taxonomic resolution. Transect data were averaged within sites to calculate mean coral cover. A total of 35 line transects were measured (Table 1).

Rugosity was measured with a rope that was aligned as closely as possible with the former reef surface at a given time (Fig. 3c, d). Rugosity is expressed as the ratio between the length of the surface-aligned rope and the shortest

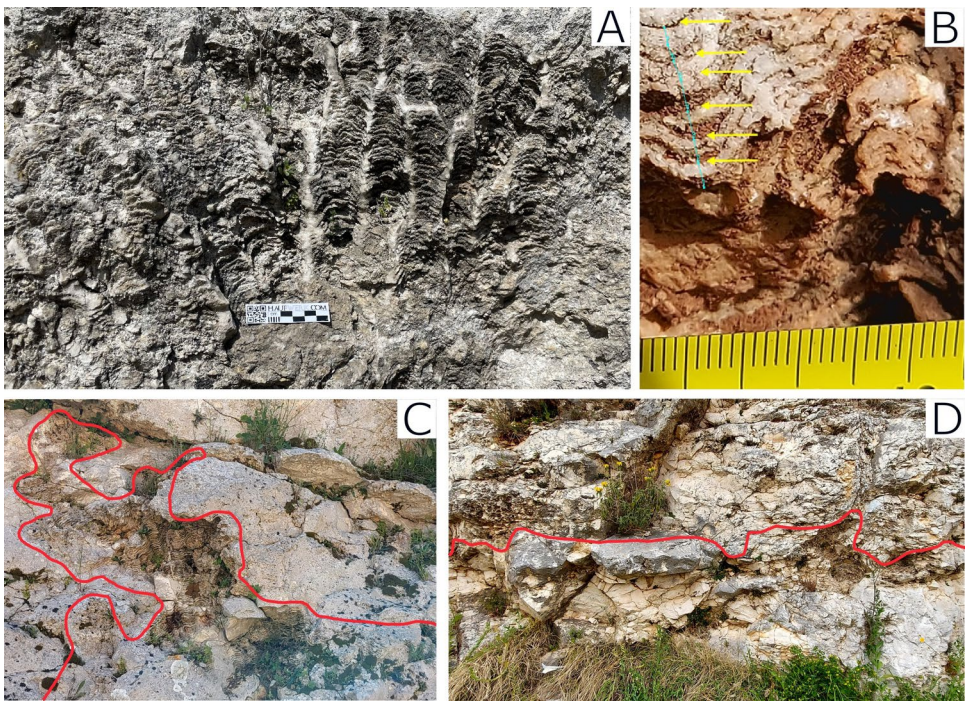

Fig. 3 Establishing census components in the field. **A**. *Porites* colony with distinct, weathering-enhanced growth bands (Chattian backreef, Vitigliano). **B**. Close-up of a *Porites* showing the inferred annual growth bands (Chattian reef front, Santa Cesarea). **C**, **D** Transects for rugosity estimates in the Chattian reef front, Santa Cesarea. **C** with high rugosity and **D** with low rugosity. The rope aligned with the former reef surface is enhanced by a thick red line for clarity

distance between the rope's endpoints. The lowest possible rugosity value is thus 1. The assessment of rugosity requires exceptional outcrop conditions with identifiable time horizons, which limited the number of sites for which P_g could be assessed (Table 1). Because empirical rugosity estimates varied substantially, we only provide reef production estimates when in-situ framework was present. Rugosity estimates were averaged within sites. We notice that our approach is close to the original reef budget approach of Perry et al. (2012), but does not consider the revised approach to measure the size and morphology of individual coral colonies instead of a transect-wide average of rugosity (Perry et al. 2015). First, not all corals had the required preservation to quantify morphology and second the great majority of corals were massive or columnar in all reef systems. Any bias from the gross-estimate of rugosity, will thus similarly affect all assessed sites.

Coral growth rates are readily accessible in outcrop (Fig. 3a,b). While the assumption that diagenetically altered growth bands are annual could not be tested, the regularity and spacing render annual cycles plausible. Reuter et al. (2005) have demonstrated how pristinely preserved annual growth bands are diagenetically transformed into coarsely recrystallized bands alternating with voids. Counterintuitively, the original high-density bands (reflecting low extension rate) are turned into voids, whereas the low-density-bands (reflecting high extension rates) are diagenetically transformed into massive calcite bands. We used a caliper to measure the distances between the bottom of a high-density growth band (weathered) and the top of a low-density growth band (resistant). A total of 1450 growth lines from 98 corals have been measured in the field. Coral growth rates are reported as genus by site means with standard errors.

Due to the lack of aragonite preservation, skeletal bulk density could not be determined in any of the corals. In general, the determination of skeletal density requires exceptional preservation (Brachert et al. 2013, 2020, 2022), which is not observed in Salento. We chose to take density estimates from the recent literature as provided by the Coral Trait Database (CTD, Madin et al. 2016). Table 2 provides details how missing values have been handled.

Diversity

Diversity data are reported as number of genera (S) and the Shannon–Wiener Index (H) where $H = -\Sigma p_i \times \ln(p_i)$. The term p_i refers to the proportional abundance of each genus to the total coral assemblage.

Results

Across all sites and corals, growth rates range between 0.01 and 1.2 cm $year^{-1}$, with an average of 0.28 cm $year^{-1}$ (median 0.24 cm $year^{-1}$). By-coral growth rates are nearly twice as high in the Oligocene (0.32 cm $year^{-1}$) as in the Miocene (0.17 cm $year^{-1}$) (Table 3). Growth rates of *Porites* were more than twice as high on average in the Oligocene (0.38 cm $year^{-1}$) as in the Miocene (0.17 cm $year^{-1}$). In the Oligocene, columnar and branching corals such as *Porites* and *Tarbellastraea* had higher growth rates than massive corals (Table 3).

Overall, we encountered 11 genera in line transects: *Actinacis*, *Astreopora*, *Caulastraea*, *Favites*, *Hydnophora*, *Montastraea*, *Pavona*, *Porites*, *Siderastrea*, *Stylophora*, and *Tarbellastraea* (Fig. 4). Diversity is highest in the Oligocene specifically in the reef front (S = 7, H = 1.29) and proximal reef slopes (S = 7, H = 1.35). *Actinacis* and *Porites* prevail in the reef front at S. Cesarea, but *Favites* is also common. Only one or two coral genera appeared in the Miocene transects, which are strongly dominated by

Table 2 Handling of missing data

Missing data	Missing data	Source
Porites	Skeletal bulk density	Mean calculated from modern data (Coral Trait Database)
Actinacis	Skeletal bulk density	No sources → same as *Porites*
Favites	Skeletal bulk density	Mean calculated from modern data of *Goniastrea* (Coral Trait Database)
	Growth rate	Mean calculated from modern data (Coral Trait Database)
Stylophora	Skeletal bulk density	Mean calculated from modern data (Coral Trait Database)
	Growth rate	Mean calculated from modern data (Coral Trait Database)
Tarbellastraea	Skeletal bulk density	Has higher density than *Porites* (Giannetti et al. 2020)
Hydnophora	Skeletal bulk density	Mean calculated from modern data (Coral Trait Database)
	Growth rate	Mean calculated from modern data (Coral Trait Database) (Morgan and Kench 2012)
Montastraea	Skeletal bulk density	Mean calculated from modern data (Coral Trait Database)
	Growth rate	Mean calculated from modern data (Coral Trait Database)

Table 3 Coral growth rates (in cm year^{-1}) at the investigated sites (means ± standard error)

Site	*Porites*	*Actinacis*	*Tarbell-astraea*	*Pavona*	*Astreopora*	Weighted mean
Oligocene back reef	0.335 ± 0.008	0.198 ±0.009	0.308 ± 0.011	0.179 ± 0.016	-	0.287 ± 0.007
Oligocene reef front	0.44 ± 0.015	0.369 ± 0.015	-	-	0.270 ± 0.018	0.363 ± 0.002
Oligocene proximal slope	0.211 ± 0.017	-	-	-	-	0.209 ± 0.009
Total Oligocene	0.381 ± 0.009	0.230 ± 0.009	0.308 ± 0.011	0.179 ± 0.016	0.270 ± 0.018	**0.317 ± 0.005**
Miocene back reef	0.142 ± 0.004	-	-	-	-	0.142 ± 0.004
Miocene reef front	0.172 ± 0.005	-	-	-	-	0.172 ± 0.005
Miocene proximal slope	0.160 ± 0.006	-	-	-	-	0.160 ± 0.006
Total Miocene	0.165 ± 0.003	-	-	-	-	**0.165 ± 0.003**

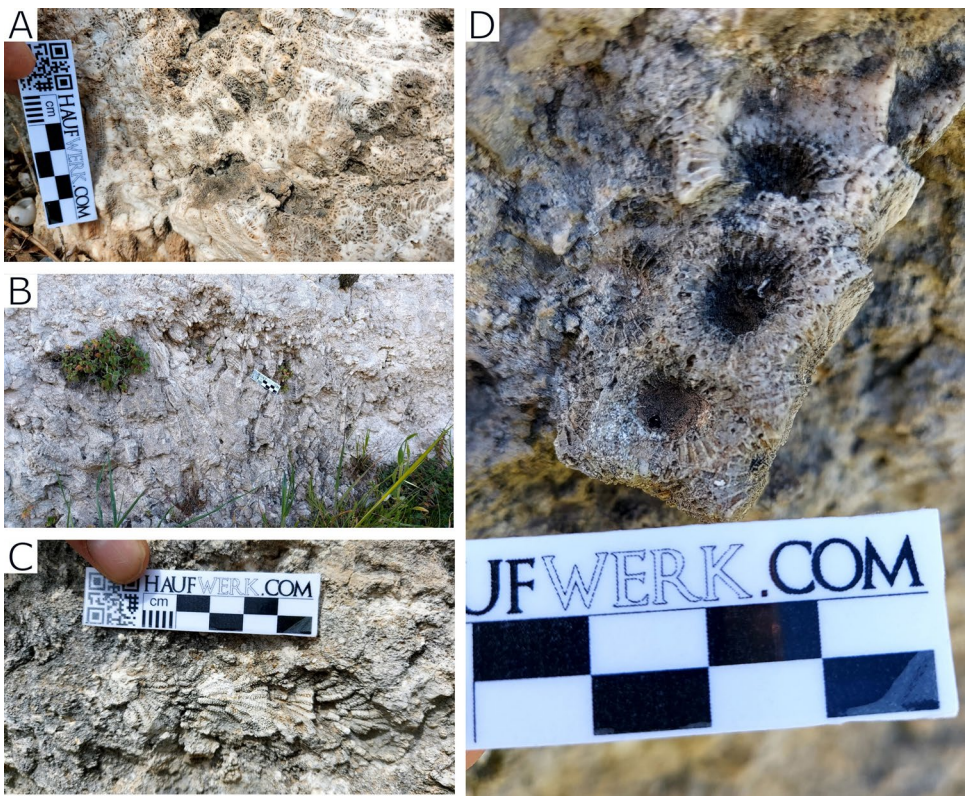

Fig. 4 Examples of corals encountered in the field. **A** *Montastraea*, **B** *Stylocoenia*, **C** *Alveopora*, **D** *Favites*

Porites. Coral abundance varies from 17% in the Miocene backreef to 56% in the Oligocene reef front at S. Cesarea.

In-situ preservation of corals only occurs at three sites, for which we identify 56 ± 2% cover at S. Cesarea (Oligocene reef front), 40 ± 3% cover at Ciolo-Gagliano (Miocene reef front), and 35 ± 4% cover at Leuca (Miocene proximal slope) (Fig. 5). Within these sites, non-coral carbonate producers (mostly coralline algae) occurred as well, but with less than 1% cover. The same applies to bioerosion. Among all 899 points in line transects of the three sites, only one hit a bivalve macroboring. Clionid borings were also observed but not encountered in line transects. The bulk of the non-coral constituents is formed by bioclastic sediment (Fig. 5).

Rugosity was highest in the Miocene proximal reef slope, but rugosity values of the Oligocene and Miocene reef fronts were nearly identical (Fig. 6). Together with the estimated skeletal bulk densities of corals, we applied Eq. (1) to compute the reefal carbonate production by site. We achieve 6.05 ± 1.31 kg $CaCO_3$ m^{-2} $year^{-1}$ in the Oligocene reef front, 1.67 ± 0.47 kg $CaCO_3$ m^{-2} $year^{-1}$ in the late Miocene reef front, and 2.48 ± 0.62 kg $CaCO_3$ m^{-2} $year^{-1}$ in the Miocene proximal slope (Fig. 7).

Discussion

Credibility of results

Since this is the first study to apply a census-based approach to fossil reefs, we need to be critical and discuss potential caveats. Annual extension rates in our study appear to be much lower than in modern reef corals, even in the same genera. For example, the average growth rate of modern *Porites* in the CTD (Madin et al. 2016) is 13.7 mm $year^{-1}$, which is more than 3 times as much as the average *Porites* growth rate in the Oligocene reef front and 8 times as much as *Porites* in the Miocene reef front (Table 3). However, published growth rates from pristine *Porites* material in the Miocene of the Mediterranean (i.e. 2–4 mm $year^{-1}$ in the Late Miocene of Crete, Reuter et al. 2005; Brachert et al. 2006) are similar to our material, suggesting that our

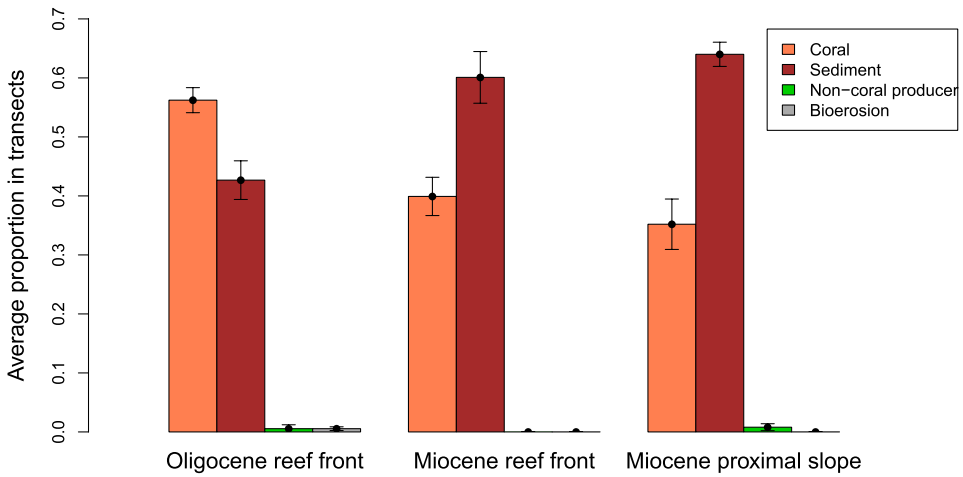

Fig. 5 Summary of transect data for sites with abundant corals in growth position. Error bars demarcate standard errors across transects within sites

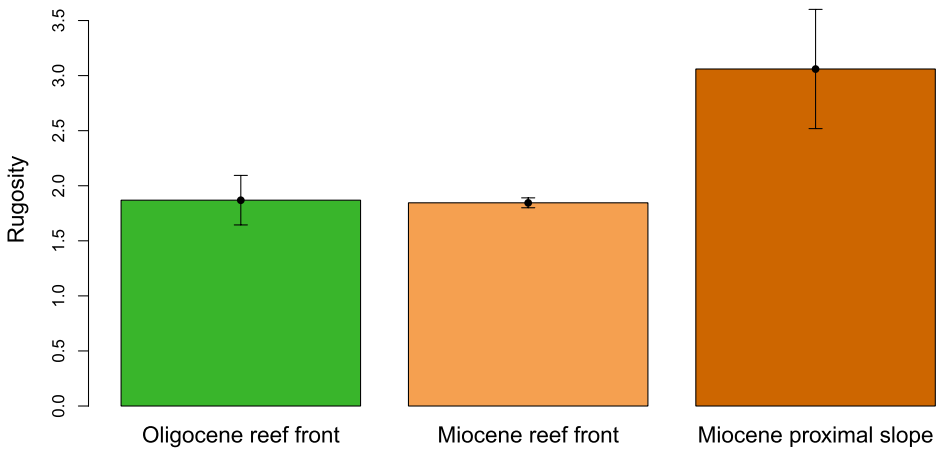

Fig. 6 Rugosity assessment for sites with reef framework. Error bars demarcate standard errors of transects within sites

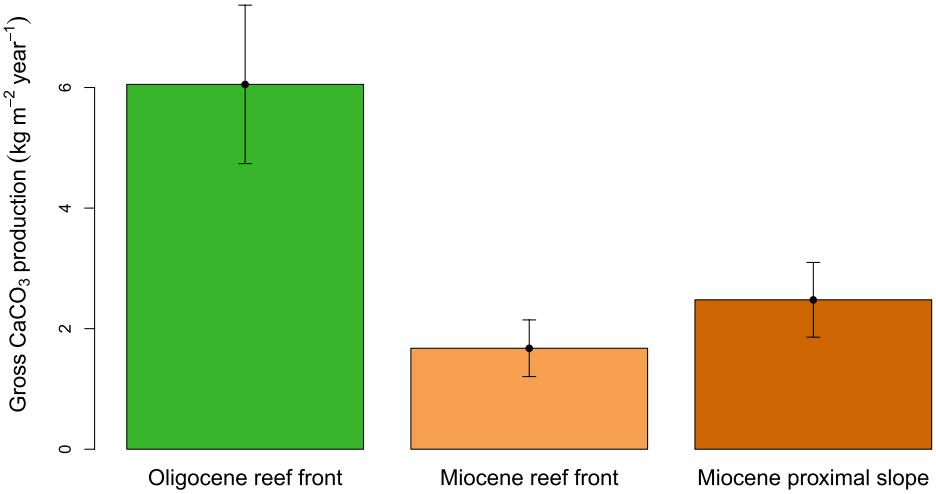

Fig. 7 Estimated gross carbonate production by site. Error bars demarcate standard errors of weighted means

measurements do represent annual growth bands and late Cenozoic coral growth rates in the Mediterranean were substantially lower than tropical growth rates today.

Given the differences in growth rates, our approach to take the missing bulk skeletal density data of our fossil corals from extant representatives may be questioned. There is usually a negative correlation between growth rate and bulk density (Brachert et al. 2016, 2020). We would thus expect higher skeletal density of slower growing specimens of the same taxon. However, we argue that the introduced bias is probably negligible. For example pristine Eocene *Astreopora* material showed both low growth rates and skeletal density (Brachert et al. 2022) substantially lower than our average assumed density values of 1.5 g cm^{-3}. While the total lack of skeletal bulk density data in our material is a major caveat, this is a caveat that will affect any studies of fossil reefs without aragonite preservation.

A final critical component of our assessment is reef rugosity. While the surfaces we measured for reef rugosity appeared like primary reef surfaces preserving biologically built relief, there is a possibility that these paleo-surfaces were enhanced by subaerial weathering rather than the biological creation of the reef framework. Some weathering is indeed apparent (Fig. 2C), but this is probably due to submarine dissolution while the reef was still actively growing. Even if weathering has increased rugosity in the paleoreefs, this would not affect the key result of a substantial decline of carbonate production from the Oligocene to the Miocene. Rugosity values are even higher on average in the Miocene than in the Oligocene (Fig. 6) due to the columnar growth forms of the monogeneric *Porites* reef transects. The inferred decline of carbonate production is thus not due to rugosity but rather due to a lower coral cover (Fig. 5) and lower coral growth rates. Future census-approaches would also benefit from applying the revised reef budget approach (Perry et al. 2015) and assess the morphology of individual coral colonies instead of gross rugosity across the entire reef.

Overall, our estimated gross carbonate production rates fall within the interquartile range of the gross carbonate production rates in modern reefs. Perry et al. (2018) estimated the reef budget of 1041 reef sites in the Caribbean and Indian Ocean and found a median gross production of 3.08 kg $CaCO_3$ m^{-2} $year^{-1}$ with the 25 percentile at 1.17 kg $CaCO_3$ m^{-2} $year^{-1}$ and the 75 percentile at 6.8 kg $CaCO_3$ m^{-2} $year^{-1}$. In spite of all uncertainties, we thus argue that our estimates of reef carbonate production are plausible. How representative they are for reefal carbonate production in the Oligocene and Miocene of the Mediterranean region is another question that is addressed in the last subsection.

Towards a full carbonate budget

To estimate a full carbonate budget, the destructive processes need to be quantified and balanced against the constructive processes. In modern reefs, bioerosion is a key destructive force supplemented by mechanical breakdown (Hubbard et al. 1990; Lange et al. 2020). Assessing again the primary data of Perry et al. (2018) and excluding gross production values below the 25 percentile, the average ratio of bioerosion to gross production is 0.71, meaning that typically 71% of gross carbonate production is removed and net production is only 29% of gross production.

The low amount of macroscopically visible bioerosion suggests that bioerosion may have been negligible unless there was a lot of hidden bioerosion or dissolution. Bioerosion appears to be very low in our sites, less than 1%. In modern reefs, the bulk of bioerosion is from superficial attack such as parrotfish (Bellwood 1995; Perry et al. 2018), which is difficult to track in fossil material. However, parrotfishes (Scarinae) only emerged in the mid-Miocene and did

not diversify before the Pliocene (Choat et al. 2012), which renders it unlikely that they affected the studied reef systems. Sea urchins are another surface bioeroding component, but they only comprise 5.5% of reef bioerosion in modern reefs.

The large proportion of bioclastic sediment in the Salento reefs might indicate mechanical breakdown as a dominant destructive agent. However, the large proportion of bioclastic sediment can only partly be attributed to mechanical breakdown of the reef framework, because the sediment contains numerous large foraminifers and cements in the Oligocene (Bosellini and Russo 1992) and *Halimeda* and smaller foraminifers in the Miocene (Bosellini et al. 2002). And even if all sediment were derived from mechanical breakdown, it is sediment that remained in the reef system and is thus not lost from the system. Also in modern reefs, more than 50% of the initial carbonate production may end up as bioclastic sediment of which more than 70% is retained in the reef (Hubbard et al. 1990).

While unknown rates of bioerosion and sediment export are currently limiting our ability to present a full carbonate budget for the fossil reefs, we argue that the difference between gross and net carbonate production was lower than in most modern reefs. Unlike some modern reefs (Perry et al. 2018), fossil reefs must have had an overall positive carbonate budget before being buried. Reefs with a negative budget are unlikely to preserve as three-dimensional geological structures because they will be transformed into rubble beds.

Was there a genuine carbonate production decline from the Oligocene into the Miocene?

Among the three sites where a full assessment was feasible, we found that the maximum carbonate production was in the Chattian reef front. The Messinian reef had substantially lower carbonate production rates, particularly in the equivalent reef front setting, where carbonate production was a 72% lower than in the Chattian. It thus appears that there was a substantial decline in carbonate production from the Oligocene into the Miocene.

This result requires further discussion given that Late Miocene reefs are well developed, particularly in the western and central Mediterranean region (Esteban 1996; Cornacchia et al. 2021). Some authors argued that the Late Miocene was the birth of modern-style coral reefs with enhanced calcification rates of reef corals due to a more efficient photosymbiosis (Pomar and Hallock 2007; Pomar et al. 2017). Oligocene reefs in contrast are known for the high coral diversity but less for extensive reef building (Bosellini 2006; Bosellini et al. 2021). For the Salento reef system, one paper even argued for a Chattian ramp situation with limited reef development (Pomar et al. 2014).

We must stress again that a census-based estimate of carbonate production provides a snapshot estimate and may not be representative of reef accretion and reef growth in the longer run (Perry et al. 2008; Perry 2011; Januchowski-Hartley et al. 2017). Therefore, more massive Messinian reef development can stem from more sustained reef growth and less erosion in spite of reduced annual calcium carbonate production.

In addition, our data are localized and may not be representative of the carbonate production of the broader reef system. The carbonate production of modern reefs varies considerably even within the same sites. For example, according to the supplementary data of Perry et al. (2018), the gross carbonate production of one site at St. Croix in the Caribbean varies between 4.0 and 12.2 kg (n = 4, mean 7.2) $CaCO_3$ m^{-2} $year^{-1}$ in the same water depth and coral facies. Because our data are already averaged across several transects, variation among should be modulated. However, given the huge variation of modern gross production rates even within larger areas, we cannot yet establish that the variation of gross carbonate production is greater in time than in space.

The drivers of our inferred Miocene decline in carbonate productions provide further insights: lower coral cover and lower coral growth rate. The significantly lower coral growth rates in the Miocene compared to the Oligocene (Table 3) allow us to question the hypothesis of an increased coral calcification in the Late Miocene suggested by Pomar and Hallock (2007). Coral cover can locally reach higher values than encountered in our transects (Bosellini et al. 2002) and there are more non-coral carbonate producers such as red and green algae (*Halimeda*), and vermetids (Bosellini 2006). As these producers have not been considered in our calculation, the actual difference in carbonate production may be less than indicated. However, the reduced coral growth rates are robust to local variation and may alone be responsible for a 53% decline in carbonate production rates (61% when just considering *Porites*).

Both the reduced diversity and the reduced coral growth in the Late Miocene are probably governed by the same environmental drivers, namely the gradual northwards shift of the Mediterranean region outside the tropical belt and closure of the seaway with the Indo-Pacific, together with global cooling (Bosellini and Perrin 2008; Perrin and Bosellini 2012, 2013). The age of the Chattian reef has been placed within the Late Oligocene Warming Event (LOWE), from which a substantial cooling towards the Late Miocene is recorded (Westerhold et al. 2020). This cooling likely negatively affected coral diversity and their growth potential.

Conclusions

New to fossil reefs, we applied a census-based approach to reconstruct the reefal carbonate production. We found the late Oligocene carbonate production values were more than three times greater than Late Miocene production values, probably due to global cooling. As Apulian reefs appear to be similarly well developed in the Oligocene and Miocene, this difference in snapshot carbonate production may have been balanced by a longer productive phase of Miocene reefs than Oligocene reefs.

A census-based approach to calcium carbonate production can likely be applied to many fossil reefs. As this approach does not suffer from the scale-dependency of similar approaches to carbonate accumulation rates, census-based carbonate budgets are a promising route to the reconstruction of reef productivity in the deep-time past.

Acknowledgements This work was supported by the Deutsche Forschungsgemeinschaft (KI 806/17–1) and is embedded in the Research Unit TERSANE (FOR 2332: "Temperature-related Stressors as a Unifying Principle in Ancient Extinctions"). We also acknowledge support from the European Union—Next Generation EU PRIN MUR 2022WEZE44 to C. Bottini: "Conservation of life on Earth: the fossil record as an unparalleled archive of ecological and evolutionary responses to past warming events". Valuable comments from reviewer Chris Perry and an anonymous reviewer as well as suggestions from editor Maurice Tucker are acknowledged.

Funding Open Access funding enabled and organized by Projekt DEAL.

Data availability Primary data (coral growth rates, line transect data, rugosity estimates) are available on Zenodo: https://doi.org/10.5281/zenodo.14210072.

References

Bellwood DR (1995) Direct estimate of bioerosion by two parrotfish species, *Chlorurus gibbus* and *C. sordidus*, on the Great Barrier Reef, Australia. Mar Biol 121:419–429. https://doi.org/10.1007/BF00349451

Bosellini FR (2006) Biotic changes and their control on Oligocene-Miocene reefs: a case study from the Apulia Platform margin (southern Italy). Palaeogeogr Palaeoclimatol Palaeoecol 241:393–409. https://doi.org/10.1016/j.palaeo.2006.04.001

Bosellini FR, Perrin C (2008) Estimating Mediterranean Oligocene-Miocene sea-surface temperatures: an approach based on coral taxonomic richness. Palaeogeogr Palaeoclimatol Palaeoecol 258:71–88. https://doi.org/10.1016/j.palaeo.2007.10.028

Bosellini FR, Russo A (1992) Stratigraphy and facies of an Oligocene fringing reef (Castro Limestone, Salento Peninsula, southern Italy). Facies 26:145–166. https://doi.org/10.1007/BF02539798

Bosellini A, Bosellini FR, Colalongo ML, Parente M, Russo A, Vescogni A (1999) Stratigraphic architecture of the Salento coast from Capo d'Otranto to S. Maria di Leuca (Apulia, southern Italy). Riv Ital Paleontol Stratigr 105:397–416. https://doi.org/10.13130/2039-4942/5382

Bosellini FR, Russo A, Vescogni A (2001) Messinian reef-building assemblages of the Salento Peninsula (southern Italy): palaeobathymetric and palaeoclimatic significance. Palaeogeogr Palaeoclimatol Palaeoecol 175:7–26. https://doi.org/10.1016/S0031-0182(01)00383-2

Bosellini FR, Russo A, Vescogni A (2002) The Messinian reef complex of the Salento Peninsula (southern Italy): stratigraphy, facies and paleoenvironmental interpretation. Facies 47:91–112. https://doi.org/10.1007/BF02667708

Bosellini FR, Vescogni A, Budd AF, Papazzoni CA (2021) High coral diversity is coupled with reef-building capacity during the Late Oligocene Warming Event (Castro Limestone, Salento Peninsula, S Italy). Rivista Ital Paleontol Stratigr 127:515–538. https://doi.org/10.13130/2039-4942/16332

Brachert TC, Reuter M, Kroeger KF, Lough JM (2006) Coral growth bands: a new and easy to use paleothermometer in paleoenvironment analysis and paleoceanography (late Miocene, Greece). Paleoceanography. https://doi.org/10.1029/2006PA001288

Brachert TC, Reuter M, Krüger S, Böcker A, Lohmann H, Mertz-Kraus R, Fassoulas C (2013) Density banding in corals: barcodes of past and current climate change. Coral Reefs 32:1013–1023. https://doi.org/10.1007/s00338-013-1056-7

Brachert TC, Reuter M, Krüger S, Klaus JS, Helmle K, Lough JM (2016) Low Florida coral calcification rates in the Plio-Pleistocene. Biogeosciences 13:4513–4532. https://doi.org/10.5194/bg-13-4513-2016

Brachert TC, Corrège T, Reuter M, Wrozyna C, Londeix L, Spreter P, Perrin C (2020) An assessment of reef coral calcification over the late Cenozoic. Earth Sci Rev 204:103154. https://doi.org/10.1016/j.earscirev.2020.103154

Brachert TC, Felis T, Gagnaison C, Hoehle M, Reuter M, Spreter PM (2022) Slow-growing reef corals as climate archives: a case study of the Middle Eocene Climatic Optimum 40 Ma ago. Sci Adv 8:eabm3875. https://doi.org/10.1126/sciadv.abm3875

Chave KE, Smith SV, Roy KJ (1972) Carbonate production of coral reefs. Mar Geol 12:123–140. https://doi.org/10.1016/0025-3227(72)90024-2

Choat JH, Klanten OS, Van Herwerden L, Robertson DR, Clements KD (2012) Patterns and processes in the evolutionary history of parrotfishes (Family Labridae). Biol J Linn Soc 107:529–557. https://doi.org/10.1111/j.1095-8312.2012.01959.x

Cornacchia I, Brandano M, Agostini S (2021) Miocene paleoceanographic evolution of the Mediterranean area and carbonate production changes: a review. Earth Sci Rev 221:103785. https://doi.org/10.1016/j.earscirev.2021.103785

Dullo W-C (2005) Coral growth and reef growth: a brief review. Facies 51:33–48. https://doi.org/10.1007/s10347-005-0060-y

Edinger EN, Limmon GV, Jompa J, Widjatmoko W, Heikoop JM, Risk MJ (2000) Normal coral growth rates on dying reefs: are coral growth rates good indicators of reef health? Mar Pollut Bull 40:404–425. https://doi.org/10.1016/S0025-326X(99)00237-4

Esteban M (1996) An overview of Miocene reefs from Mediterranean area: general trends and facies models. SEPM ConceptsSedimentol 5:3–53. https://doi.org/10.2110/csp.96.01.0003

Giannetti A, Falces-Delgado S, Baeza-Carratalá JF (2020) Bioerosion pattern in a nearshore setting as a tool to disentangle multiphase transgressive episodes. Palaeogeogr Palaeoclimatol Palaeoecol 554:109820. https://doi.org/10.1016/j.palaeo.2020.109820

Hubbard DK, Miller AI, Scaturo D (1990) Production and cycling of calcium carbonate in a shelf-edge reef system (U.S. Virgin Islands): applications to the nature of reef systems in the fossil record. J Sediment Petrol 60:335–360. https://doi.org/10.1306/212F9197-2B24-11D7-8648000102C1865D

Januchowski-Hartley FA, Graham NAJ, Wilson SK, Jennings S, Perry CT (2017) Drivers and predictions of coral reef carbonate budget trajectories. Proc R Soc B Biol Sci 1:1. https://doi.org/10.1098/rspb.2016.2533

Jokiel PL, Rodgers KS, Brown EK, Kenyon JC, Aeby G, Smith WR, Farrell F (2015) Comparison of methods used to estimate coral cover in the Hawaiian Islands. PeerJ 3:e954. https://doi.org/10.7717/peerj.954

Kemp DB (2012) Stochastic and deterministic controls on stratigraphic completeness and fidelity. Int J Earth Sci 101:2225–2238. https://doi.org/10.1007/s00531-012-0784-1

Lange ID, Perry CT, Alvarez-Filip L (2020) Carbonate budgets as indicators of functional reef "health": a critical review of data underpinning census-based methods and current knowledge gaps. Ecol Ind 110:105857. https://doi.org/10.1016/j.ecolind.2019.105857

Lough JM (2008) Coral calcification from skeletal records revisited. Mar Ecol Prog Ser 373:257–264. https://doi.org/10.3354/meps07398

Lough JM, Cooper TF (2011) New insights from coral growth band studies in an era of rapid environmental change. Earth Sci Rev 108:170–184. https://doi.org/10.1016/j.earscirev.2011.07.001

Madin JS, Anderson KD, Andreasen MH, Bridge TCL, Cairns SD, Connolly SR, Darling ES, Diaz M, Falster DS, Franklin EC, Gates RD, Harmer AMT, Hoogenboom MO, Huang D, Keith SA, Kosnik MA, Kuo C-Y, Lough JM, Lovelock CE, Luiz O, Martinelli J, Mizerek T, Pandolfi JM, Pochon X, Pratchett MS, Putnam HM, Roberts TE, Stat M, Wallace CC, Widman E, Baird AH (2016) The Coral Trait Database, a curated database of trait information for coral species from the global oceans. Sci Data 3:160017. https://doi.org/10.1038/sdata.2016.17

Mewis H, Kiessling W (2013) Environmentally controlled succession in a late Pleistocene coral reef (Sinai, Egypt). Coral Reefs 32:49–58. https://doi.org/10.1007/s00338-012-0968-y

Morgan KM, Kench PS (2012) Skeletal extension and calcification of reef-building corals in the central Indian Ocean. Mar Environ Res 81:78–82. https://doi.org/10.1016/j.marenvres.2012.08.001

Perrin C, Bosellini FR (2012) Paleobiogeography of scleractinian reef corals: Changing patterns during the Oligocene-Miocene climatic transition in the Mediterranean. Earth Sci Rev 111:1–24. https://doi.org/10.1016/j.earscirev.2011.12.007

Perrin C, Bosellini FR (2013) The Late Miocene coldspot of z-coral diversity in the Mediterranean: patterns and causes. CR Palevol 12:245–255. https://doi.org/10.1016/j.crpv.2013.05.010

Perrin C, Kiessling W (2010) Latitudinal trends in Cenozoic reef patterns and their relationship to climate. In: Mutti M, Piller Werner E, Betzler C (eds) Carbonate Systems during the Oligocene-Miocene climatic transition. Wiley-Blackwell, Oxford, pp 17–34. https://doi.org/10.1002/9781118398364.ch2

Perry CT (2011) Carbonate budgets and reef framework accumulation. In: Hopley D (ed) Encyclopedia of modern coral reefs: structure, form and process. Springer, Dordrecht, pp 185–190. https://doi.org/10.1007/978-90-481-2639-2_53

Perry C, Spencer T, Kench P (2008) Carbonate budgets and reef production states: a geomorphic perspective on the ecological phase-shift concept. Coral Reefs 27:853–866. https://doi.org/10.1007/s00338-008-0418-z

Perry CT, Edinger EN, Kench PS, Murphy GN, Smithers SG, Steneck RS, Mumby PJ (2012) Estimating rates of biologically driven coral reef framework production and erosion: a new census-based carbonate budget methodology and applications to the reefs of Bonaire. Coral Reefs 31:853–868. https://doi.org/10.1007/s00338-012-0901-4

Perry CT, Murphy GN, Graham NAJ, Wilson SK, Januchowski-Hartley FA, East HK (2015) Remote coral reefs can sustain high growth potential and may match future sea-level trends. Sci Rep 5:18289. https://doi.org/10.1038/srep18289

Perry CT, Alvarez-Filip L, Graham NAJ, Mumby PJ, Wilson SK, Kench PS, Manzello DP, Morgan KM, Slangen ABA, Thomson DP, Januchowski-Hartley F, Smithers SG, Steneck RS, Carlton R, Edinger EN, Enochs IC, Estrada-Saldívar N, Haywood MDE, Kolodziej G, Murphy GN, Pérez-Cervantes E, Suchley A, Valentino L, Boenish R, Wilson M, Macdonald C (2018) Loss of coral reef growth capacity to track future increases in sea level. Nature 558:396–400. https://doi.org/10.1038/s41586-018-0194-z

Pomar L, Hallock P (2007) Changes in coral-reef structure through the Miocene in the Mediterranean province: adaptive versus environmental influence. Geology 35:899–902. https://doi.org/10.1130/G24034A.1

Pomar L, Mateu-Vicens G, Morsilli M, Brandano M (2014) Carbonate ramp evolution during the Late Oligocene (Chattian), Salento Peninsula, southern Italy. Palaeogeogr Palaeoclimatol Palaeoecol 404:109–132. https://doi.org/10.1016/j.palaeo.2014.03.023

Pomar L, Baceta JI, Hallock P, Mateu-Vicens G, Basso D (2017) Reef building and carbonate production modes in the west-central Tethys during the Cenozoic. Mar Pet Geol 83:261–304. https://doi.org/10.1016/j.marpetgeo.2017.03.015

Reuter M, Brachert TC, Kroeger KF (2005) Diagenesis of growth bands in fossil scleractinian corals: identification and modes of preservation. Facies 51:155–168. https://doi.org/10.1007/s10347-005-0064-7

Sadler PM (1981) Sediment accumulation rates and the completeness of stratigraphic sections. J Geol 89:569–584. https://doi.org/10.1086/628623

Schlager W (1981) The paradox of drowned reefs and carbonate platforms. Geol Soc Am Bull 92:197–211. https://doi.org/10.1130/0016-7606(1981)92%3c197:TPODRA%3e2.0.CO;2

Schlager W (1999) Scaling of sedimentation rates and drowning of reefs and carbonate platforms. Geology 27:183–186. https://doi.org/10.1130/0091-7613(1999)027%3c0183:SOSRAD%3e2.3.CO;2

Westerhold T, Marwan N, Drury AJ, Liebrand D, Agnini C, Anagnostou E, Barnet JSK, Bohaty SM, De Vleeschouwer D, Florindo F, Frederichs T, Hodell DA, Holbourn AE, Kroon D, Lauretano V, Littler K, Lourens LJ, Lyle M, Pälike H, Röhl U, Tian J, Wilkens RH, Wilson PA, Zachos JC (2020) An astronomically dated record of Earth's climate and its predictability over the last 66 million years. Science 369:1383–1387. https://doi.org/10.1126/science.aba6853